

---

EFDA-JET-CP(05)02-16

T. Hellsten, M. Laxåback, T. Bergkvist, T. Johnson, F. Meo, F. Nguyen, C.C. Petty,  
M. Mantsinen, G. Matthews, J.-M. Noterdaeme, T. Tala, D. Van Eester, P. Andrew,  
P. Beaumont, V. Bobkov, M. Brix, J. Brzozowski, L.-G. Eriksson, C. Giroud, E.  
Joffrin, V. Kiptily, J. Mailloux, M.-L. Mayoral, I. Monakhov, R. Sartori, A. Staebler,  
E. Rachlew, E. Tennfors, A. Tuccillo, A. Walden, K.-D. Zastrow  
and JET EFDA contributors

# On the Parasitic Absorption in FWCD Experiments in JET ITB Plasmas



# On the Parasitic Absorption in FWCD Experiments in JET ITB Plasmas

T. Hellsten<sup>1</sup>, M. Laxåback<sup>1</sup>, T. Bergkvist<sup>1</sup>, T. Johnson<sup>1</sup>, F. Meo<sup>2</sup>, F. Nguyen<sup>3</sup>, C.C. Petty<sup>4</sup>,  
M. Mantsinen<sup>5</sup>, G. Matthews<sup>7</sup>, J.-M. Noterdaeme<sup>8,12</sup>, T. Tala<sup>6</sup>, D. Van Eester<sup>9</sup>,  
P. Andrew<sup>7</sup>, P. Beaumont<sup>7</sup>, V. Bobkov<sup>8</sup>, M. Brix<sup>8</sup>, J. Brzozowski<sup>1</sup>, L.-G. Eriksson<sup>3</sup>,  
C. Giroud<sup>7</sup>, E. Joffrin<sup>3</sup>, V. Kiptily<sup>7</sup>, J. Mailloux<sup>7</sup>, M.-L. Mayoral<sup>7</sup>, I. Monakhov<sup>7</sup>,  
R. Sartori<sup>10</sup>, A. Staebler<sup>8</sup>, E. Rachlew<sup>1</sup>, E. Tennfors<sup>1</sup>, A. Tuccillo<sup>11</sup>, A. Walden<sup>7</sup>,  
K.-D. Zastrow<sup>7</sup> and JET EFDA contributors\*

<sup>1</sup>Association VR-Euratom, Sweden,

<sup>2</sup>Association Euratom-Risø, National Laboratory, Denmark

<sup>3</sup>Association Euratom-CEA, CEA-Cadarache, France

<sup>4</sup>General Atomics, San Diego, USA

<sup>5</sup>HUT, Association Euratom-Tekes, Finland

<sup>6</sup>VTT Processes, Association Euratom-Tekes, Finland

<sup>7</sup>EURATOM/UKAEA Fusion Association, Culham Science Centre, Abingdon, OX14 3DB, UK

<sup>8</sup>Max-Planck-Institut für Plasmaphysik, EURATOM Association, Garching, Germany,

<sup>9</sup>LPP-ERM/KMS, Association Euratom-Belgian State, Belgium,

<sup>10</sup>EFDA CSU-Garching, Germany

<sup>11</sup>ENEA, Association Euratom-ENEA, Italy,

<sup>12</sup>EESA Department, University of Gent, Belgium,

\* See annex of J. Pamela et al, "Overview of JET Results",

(Proc. 20th IAEA Fusion Energy Conference, Vilamoura, Portugal (2004)).

Preprint of Paper to be submitted for publication in Proceedings of the  
EPS Conference,

(Tarragona, Spain 27th June - 1st July 2005)

"This document is intended for publication in the open literature. It is made available on the understanding that it may not be further circulated and extracts or references may not be published prior to publication of the original when applicable, or without the consent of the Publications Officer, EFDA, Culham Science Centre, Abingdon, Oxon, OX14 3DB, UK."

"Enquiries about Copyright and reproduction should be addressed to the Publications Officer, EFDA, Culham Science Centre, Abingdon, Oxon, OX14 3DB, UK."

## ABSTRACT.

Fast Wave Current Drive (FWCD), has been performed in JET plasmas with internal transport barriers, ITBs. The heating during the FWCD is strongly degraded compared to dipole heating. The FWCD has only a small effect on the central current density. The main reasons are the parasitic absorption of RF power, the strongly inductive nature of the plasma and the interplay between the fast wave driven current and bootstrap current.

## 1. EXPERIMENTAL RESULTS

Fast wave current drive experiments have been carried out in hot low density ITB plasmas in JET with  $T_e \approx 8\text{keV}$ ,  $T_i \approx 12\text{keV}$ ,  $n_e \approx 2.4 \times 10^{19}\text{m}^{-3}$ ,  $B_0 = 3.45\text{T}$  and  $I_p = 2\text{MA}$ . Strongly reversed magnetic shear were produced with 2-2.5MW LHCD, which was switched off when around 13MW of NBI and up to 6MW of ICRF power at 37MHz were applied. The time sequence of the coupled power, central electron and ion temperatures, density and BeII radiation can be seen in Fig.1. Before  $t = 7.4\text{s}$  the outermost edge of the internal transport barrier was located at about  $R = 3.25\text{m}$ ,  $r/a = 0.28$ . At  $t = 7.4\text{s}$   $q_{\text{min}}$  reached 2 and the barrier expanded, following the outer  $q = 2$  surface to  $3.45\text{m}$ ,  $r/a = 0.5$  resulting in an increase of the ion temperature above  $20\text{keV}$ . To avoid disruption the NBI power was stepped down when the neutron yield exceeded a preset level.

For FWCD the antennas were phased at  $+90^\circ$  and  $-90^\circ$  producing asymmetric toroidal mode spectra peaked at  $n_\Delta \approx +15$  and  $n_\Delta \approx -15$ , respectively. The heating performances of the FWCD experiments were compared to two reference discharges using dipole phasing at 37MHz, (Pulse No's: 60667 with 2.9MW and 60673 with 3.1MW) and one using H-minority heating with  $+90^\circ$  at 51MHz (Pulse No: 58682 with 4.4MW). Dipole phasing produces symmetric spectra peaked at  $n_\Delta \approx \pm 25$ . The reference scenarios had better heating than FWCD as can be seen in Fig.2, where the central electron temperature and diamagnetic energy are compared. Square-wave modulations of the RF-power were performed to measure the direct electron heating from Fourier and break-in-slope analyses of the time resolved ECE temperature profiles. Profiles of direct electron heating are shown in Fig.3, which were quite similar despite the different amount of RF power. The heating efficiency was compared for a triple of discharges, Pulse No's: 60663 with  $+90^\circ$ , 60664 with  $-90^\circ$  and 60667 with dipole heating with different levels of RF power, 4.6MW, 5.8MW and 2.9MW, respectively producing similar electron temperatures and densities. The heating efficiency for  $-90^\circ$  phasing was reduced to about 50% and for  $+90^\circ$  to about 60% compared to the dipole phasing. The single pass damping of the direct electron absorption was for FWCD about 2% and slightly less for the dipole. The single pass damping for the reference scenario Pulse No: 58682 with  $n_H/n_D = 0.06$  had a single pass damping of about 60%. A part of the power was parasitically damped by residual  $^3\text{He}$  ions, whose presence was confirmed by several methods:  $\gamma$ -rays, fast energy content and ICE from  $^3\text{He}$  ions. The  $^3\text{He}$  concentration was estimated to be around 0.1%, which gave a total single pass damping in the range 3–7% with the lowest value for  $-90^\circ$ . From the balance between the energy delivered by the heating systems, including ohmic heating and excluding beam shine-through, and the energy delivered to the divertor, measured with 6

thermocouplers, and radiated from the plasma, measured with a bolometer camera, it was found that for  $\pm 90^\circ$  phasings a significant fraction of the RF power was not absorbed and transferred to the bulk plasma. For discharges dominated by ICRH the method offers a good measure of the lost power, as for Pulse No: 58680 with  $+90^\circ$  at 37MHz without NBI; 14MJ of energy could not be accounted for, corresponding to  $48\pm 13\%$  of the injected RF energy. For the reference discharge with hydrogen minority heating at 51MHz with  $+90^\circ$  phasing only 7% of the total power could not be accounted for.

In order to assess the level of sputtering or arcing taking place at the antenna Faraday screens and limiters, visible light spectrometers were used to study the intensity in the CIV and BeII lines. For the reference discharges with dipole phasing or hydrogen minority heating a steady BeII line radiation intensity of the order of  $3\times 10^{12}$  photons/s/cm<sup>2</sup>/sr was observed with the spectrometers viewing through the divertor, Fig.4. For the FWCD experiments with  $\pm 90^\circ$  phasings the radiation intensity was much larger and varied strongly during the pulses with large spikes, similar to those identified as arcs caused by rectified RF-sheath potentials during monopole heating for large misalignment angles between the magnetic field and Faraday screen [1] and with different phasing, monopole and dipole, of adjacent antennas [2].

A small but clear difference in the central current density, measured with the polarimeter, could be seen for the FWCD for the pair of discharges with  $\pm 90^\circ$  that had similar temperatures and densities in the early part of the main heating phase,  $4 < t < 6$ s, which because of the similar plasma parameters is not expected to be caused by different current diffusion rates. The driven currents were calculated with the LION code [3] with the power normalised so that the calculated power absorbed on electrons by TTMP/ELD agreed with that measured, which for Pulse No: 60665 with  $+90^\circ$  was 0.8MW and for Pulse No: 60664 with  $-90^\circ$  was 1MW, yielding driven currents of -55kA and 70 kA respectively. The effect of the current drive on the evolution of the central plasma current was simulated with the JETTO code [4]. At  $t=6$ s, the total difference in the calculated central current densities was only between 10kA/m<sup>2</sup> and 40kA/m<sup>2</sup> between co and counter current drive much smaller than the difference in measured central current densities, which was around 100kA/m<sup>2</sup>, indicating that poloidal flux diffusion takes place on a faster time scale than that by neo-classical resistivity.

## 2. CONCLUSIONS AND DISCUSSIONS

Clear differences in the heating efficiency with respect to the antenna phasing and single pass damping were seen; the dipole phasing had the highest heating efficiency, comparable to hydrogen minority heating with  $+90^\circ$  having 60% single pass damping. The lower heating efficiency of the  $\pm 90^\circ$  phasings, the strong increase of the BeII and CIV line radiation and unaccountable losses are qualitatively consistent with increased losses for weak single pass damping produced by rectified RF-sheath potentials at the antenna, which can be significant even for small misalignment angles between the magnetic field and Faraday screen [5], which in these experiments was around  $7^\circ$ . Smaller differences in heating between  $+90^\circ$  and  $-90^\circ$  are consistent with the effect of the difference in single pass damping of residual <sup>3</sup>He ions caused RF-induced spatial transport.

## REFERENCES

- [1]. M. Bures, et al Nuclear Fusion **32** (1992)1139
- [2]. D.A. D'Ippolito, et al Nuclear Fusion **42** (2002)1357
- [3]. L. Villard, et al Computer Physics Reports, **4** (1986)95 and Nuclear Fusion **35**(1995)1173
- [4]. T. Tala, et al Nuclear Fusion **40** (2000)1635
- [5]. T. Hellsten, and M. Laxåback, Physics of Plasmas **12** (2005)032505

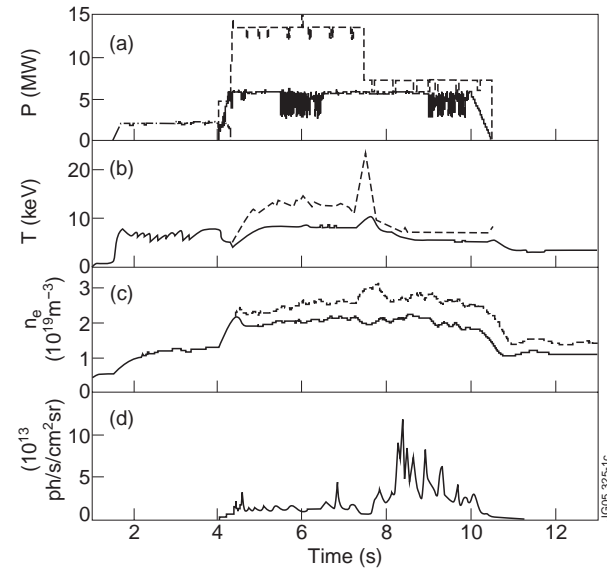


Figure 1: Time traces for Pulse No: 60664. (a) NBI, ICRF and LHCD power, (b) central electron,  $T_e$ , ion  $T_i$ , temperature, (c) on axis and volume averaged electron density,  $n_e$  and (d) BeII line radiation intensity.

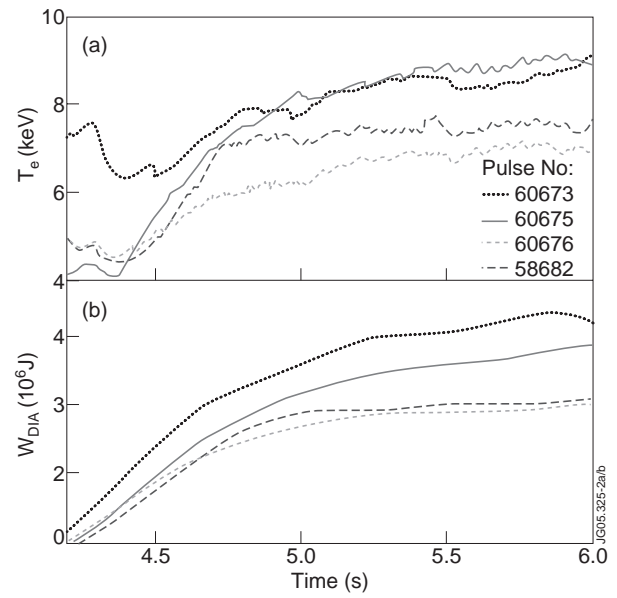


Figure 2: (a) Central electron temperatures and (b) diamagnetic energy, for Pulse No's: 58682 with 4.4MW +90° 51MHz, 60673 with 3.1MW dipole, 60675 with 5.2MW +90° and 60676 with 5.3MW -90°.

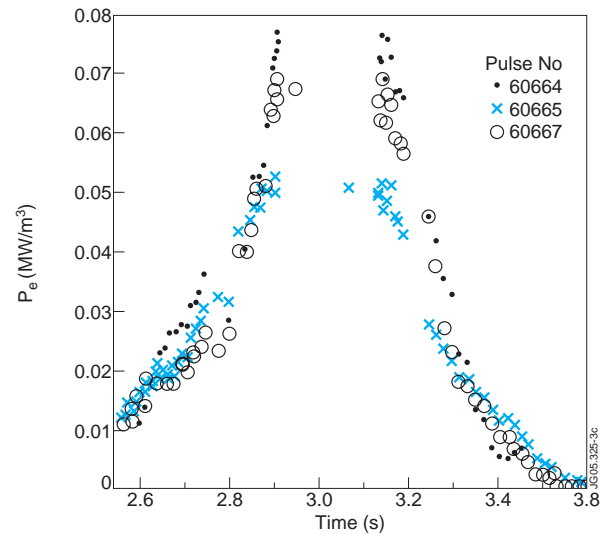


Figure 3: Power deposition by direct electron heating obtained with modulation between 5.5 and 6.5s for Pulse No's: 60664 with 5.3MW -90°, 60665 with 4.8MW +90° and 60667 with 2.9MW dipole.

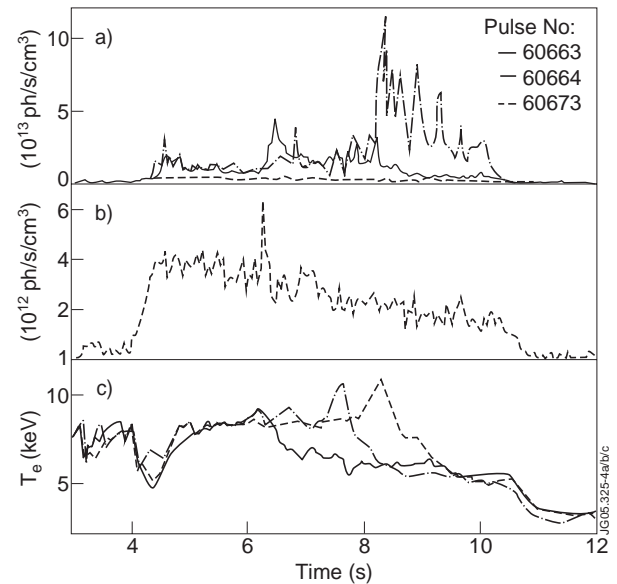


Figure 4: (a) and (b) BeII line radiation intensity for a sight line passing through the inner divertor (c) central electron temperature for Pulse No's: 60663 (+90°), 60664 (-90°) and 60673 (dipole).